Transient Temperature Distribution in a Sheet Metal by Low-Energy Laser Scanning

Yinchun Wang *, Yuren Wang

Institute of Mechanics, Chinese Academy of Sciences, 15 Beisihuanxi Road, Beijing 100080, China
e-mail: weasky@hotmail.com

Abstract Low-energy laser-heating techniques are widely used in engineering applications such as, thin film deposition, surface treatment, metal forming and micro-structural pattern formation. In this paper, under the conditions of ignoring the thermo-mechanical coupling, a numerical simulation on the spatial and temporal temperature distribution in a sheet metal produced by the laser beam scanning in virtue of the finite element method is presented. Both the three-dimensional transient temperature field and the temperature evolution as a function of heat penetrating depth in the metal sheet are calculated. The temperature dependence of material properties was taken into account. It was shown that, after taking the temperature dependence of the material absorbance effect into consideration, the temperature change rate along the scanning direction and the temperature maximum were both increased.

Key words: FEM simulation, temperature distribution, laser scanning

INTRODUCTION

A laser beam has been widely used in science and engineering areas, such as cutting, welding, surface treatment etc [1-6]. In addition to them, Laser-forming as a springback-free and noncontact forming technique [1] has been widely investigated over the last decade. Laser-induced surface acoustic waves in a layered structure has been discovered [2], and a new technique of low-energy laser scanning has been developed to get ordered ridges pattern in thin films which is useful for the fabrication of optical devices such as optical sensors [3]. However, all of these processes were governed by the same mechanism, which is named the thermal gradient mechanism [4] due to the absorption of laser energy. Therefore, the correct prediction of the temperature distribution in materials by laser-heating is promising and emergent.

The temperature field induced by laser-heating has been studied semi-analytically by several authors [5-7]. However, the nonlinear variation of material properties and coupling with thermo-mechanical process make the dynamic process very complex.The numerical simulation is a better way to isolate the effects of the different interaction processes and have a good insight into the mechanism for a complicated dynamic process. Ji and Wu [4] used FEM to simulate three-dimensional temperature fields with a moving heat source and temperature-dependent thermal properties. Yao [8] compared his numerical results of the thermal field in laser melting process with the experimental data. Nevertheless, none of their works have considered the temperature dependence of the material absorbance.

In this paper, we presented a numerical model to analyze the spatial and temporal temperature distribution in a metal sheet induced by the laser beam scanning in virtue of the finite element method. The dependences of temperature on time in different depths are also studied. The present work was focused on the study of the influence on the temperature field when the temperature dependence of the material absorbance was embedded in the calculation. The study will be helpful for the correct construction of the thermal field in the low-energy laser processing.

MATHEMATICAL AND FEA MODEL

1. Governing equations Considering a laser beam with a rectangular or square spot-shape whose area is A, and total power P, moving on a sheet metal at a constant velocity v along the x-axis, the phenomena involved can be described by two different mathematical approaches [9]. Here we used the approach which considers the laser beam as an external heat flux impinging perpendicularly on the material's surface ($z = 0$) [10]. The governing equation for the three-dimensional transient temperature field in a isotropic medium with a temperature-dependant thermal conductivity K can be rewritten as [11]:

$$\rho(T)c(T)\frac{\partial T}{\partial t} + v\rho(T)c(T)\frac{\partial T}{\partial x}$$
$$= \frac{\partial}{\partial x}\left(k_x \frac{\partial T}{\partial x}\right) + \frac{\partial}{\partial y}\left(k_y \frac{\partial T}{\partial y}\right) + \frac{\partial}{\partial z}\left(k_z \frac{\partial T}{\partial z}\right) + \text{source} \tag{1}$$

Where T is the temperature, which is a function of x, y, z and time t; ρ is the density of the material; k_x, k_y and k_z are the thermal conductivity in the x, y, and z directions respectively; c is the specific heat of the material. All of the above properties are functions of T, and the source term is expressed as heat generation per unit volume.

The convection term in Eq. (1) leads to the simultaneous occurrence of terms of both parabolic and hyperbolic nature [11], and solving such equations by the FEM is rather difficult, especially for scanning along a curve. However, in most of the low-energy laser-material interaction processes without induction of the melting of the substrate material, there is no phase change or heat generation (noticed that the laser is considered as a external heat flux) and hence, the source term can be omitted in Eq. (1). The convection term can also be neglected because it is much smaller than the heat-transfer terms [4]. In addition, on the assumption that the material has an isotropically thermal conductivity, Eq. (1) can be simplified as:

$$\rho(T)c(T)\frac{\partial T}{\partial t} = \frac{\partial}{\partial x}\left(k(T) \frac{\partial T}{\partial x}\right) + \frac{\partial}{\partial y}\left(k(T) \frac{\partial T}{\partial y}\right) + \frac{\partial}{\partial z}\left(k(T) \frac{\partial T}{\partial z}\right) \tag{2}$$

Where $T = T(\vec{r},t)$, it's a typical parabolic equation which can be easily solved using the finite element method under the following initial and boundary conditions:

$$\begin{cases} T\big|_{t=0} = T_0, & \text{the initial condition} \\ k\frac{\partial T}{\partial z}\bigg|_{z=0} = -\alpha P / A, & \text{where both } x \text{ and } y \text{ lies in the focused laser spot.} \\ k\frac{\partial T}{\partial n} = 0, & \text{where n expresses the direction of the surface.} \end{cases} \tag{3}$$

Where α is the absorbtivity of the material.

2. Finite Element Model The basic FEM equations for the thermal problem can be derived from the Eq. (2) and Eq. (3):

$$[C]\{\dot{T}\} + [K_T]\{T\} = \{Q\} \tag{4}$$

Where $[C] = \int_V \rho c[N][N]^T \,\mathrm{d}V$ is the heat capacity matrix, $[N]$ is the shape function matrix,

$[K_T] = \int_V k[B][B]^T \,\mathrm{d}V$ is the heat conduction matrix, $\{T\}$ and $\{\dot{T}\}$ are the nodal temperature vector and

nodal temperature change rate vector, respectively. $\{Q\}$ is the heat flux vector.

In the FEM analyses, the finite element code ANSYS was used to calculate the temperature field. An implicit transient thermal analysis was performed. The full model was calculated for the non-symmetric problem, as shown in Fig.1. It is assumed that the sheet is flat and free of residual stresses. Because of the high temperature and temperature gradients around the laser path, a dense mesh is necessary . In order to limit the total number of elements in the simulation, a coarse mesh was used outside the primary processing region. The elements were the thermal analysis element SOLID70 (eight-node 3-D thermal solid with thermal conduction, and convection, and material nonlinearities). An ANSYS Parametric Design Language (APDL) was used to model the moving heating laser. The total elements are 13400, i.e., 40 elements along the x-direction (in length, the scanning direction)$\times 67$ elements along the y-direction (in width)$\times 5$ elements along the z-direction (in thickness). The calculation region has three dimensional scales of 20 mm (length)$\times 20$ mm(width)$\times 1.5$ mm(thickness).

A mesh refinement test was performed. If double of the elements are used in each direction, the temperature distribution and history are almost not affected, but the computer time needed increasing dramatically, with the difference between the peak values of the temperature less than 5 K.
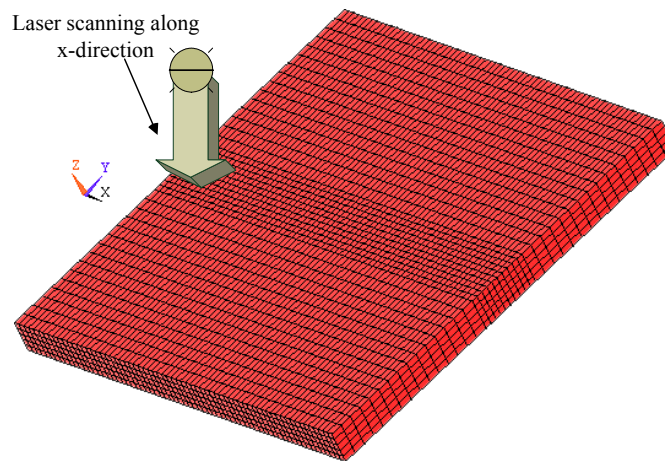

Fig. 1 The mesh of the FEM model (40×67×5)

NUMERICAL RESULTS AND DISCUSSION

1. Comparative study with previous results Before doing the laser scanning heating simulation, cases of previous studies are calculated to confirm the correctness of our FEM model. Considering the radiation effect, Ji [4] studied the temperature field of a 08 steel sheet; using the same parameters presented in Ji's paper, but without convection and radiation heat loss effects (in our model, to concentrate on the temperature dependence of the absorbtivity's influnces, no convection and radiation effects are considered.), our FEM model was employed to solve the same problem. Figure 2 shows both Ji's results for a half of the sheet and our results for a full steel sheet. It can be seen that the two calculated results are in good agreement, apart from the maximum temperature of ours being larger than theirs probably due to consideration for the convection and radiation heat loss in Ji's analysis. Our model are also compared with semi-analytical results calculated by Cheng [7], because there's no information on the geometrical parameters used in their analysis, we can only say that the temperature distribution's shapes are in good agreement.

2. Numerical results and discussion   Based on the model described above, the scanning-laser heated process on 304 stainless steel was studied. The dimensions of the sheet are 20 mm (length) $\times$ 20 mm(width) $\times$ 1.5 mm(thickness); the laser power is 1000 W and the spot area is 3×3 mm^2, with a scanning velocity 50 mm/s; the physical property parameters of 304 stainless steel [12] are adopted in our simulations and are listed in Table 1, together with the temperature dependence of the steel's absorbtivity [13].
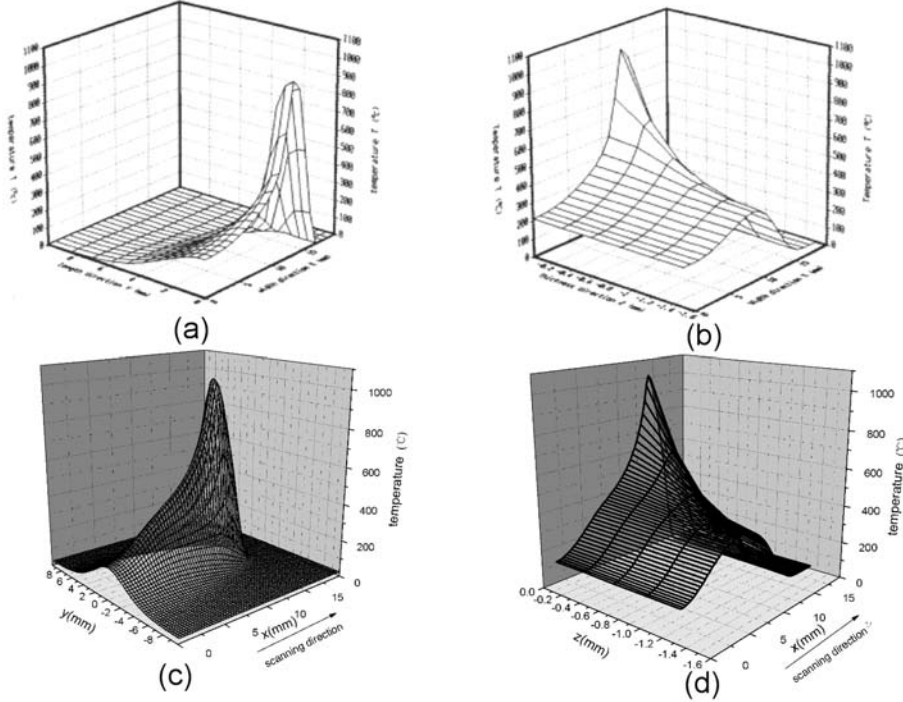

Fig. 2 Temperature distributions: (a) in (xoy) plane for a half of the sheet from Ji's model; (b) in (xoz) plane for a half of the sheet from Ji's model; (c) in (xoy) plane for the sheet calculated from our model; (d) in (xoz) plane for the sheet calculated from our model.

Table 1. Thermal parameters of 304 stainless steel used in our calculation

$T(^{\circ}C)$	0	100	500	1000	1200
$k\,(W(mm \cdot ^{\circ}C)^{-1})$	0.01522	0.01654	0.02185	0.02848	0.02848
$\rho c\,(J(mm^3 \cdot ^{\circ}\,C)^{-1})$	0.00337	0.00414	0.00462	0.00521	0.00524
α	-	0.110	0.117	0.135	0.148

In the simulation, all of the physical parameters at each temperature are determined by interpolation except the absorbtivity stepwise changed. Ignoring the "side effect" (when laser spot reaches the edge of the sheet, the peak temperature grows higher than that in the middle which is due to the small heat conduction near the border of the sheet), the 3-D transient temperature field reaches a quasi-steady state after scanning a distance of about 2 spots. In this paper, if not mentioned, we only present the results at t =0.222 s. Fig.3 illustrated the temperature distribution in *xoy* plane and *yoz* plane.Figure 3(a) indicated that there is a pre-heated zone localized in a very small region because of the low thermal conductivity of the steel in front of the laser spot. Another feature is that a "tail" exists behind the spot because of detarded heat diffusion into the metal substrate. The peak values of the temperature are not at the center of the laser spot, but at the "wheel" of the center. It's evident from Fig. 3(b) that there is a strong temperature gradient along

both x and z axises. It was well accepted that a large temperature gradient results in the metal sheet deformation in laser forming.
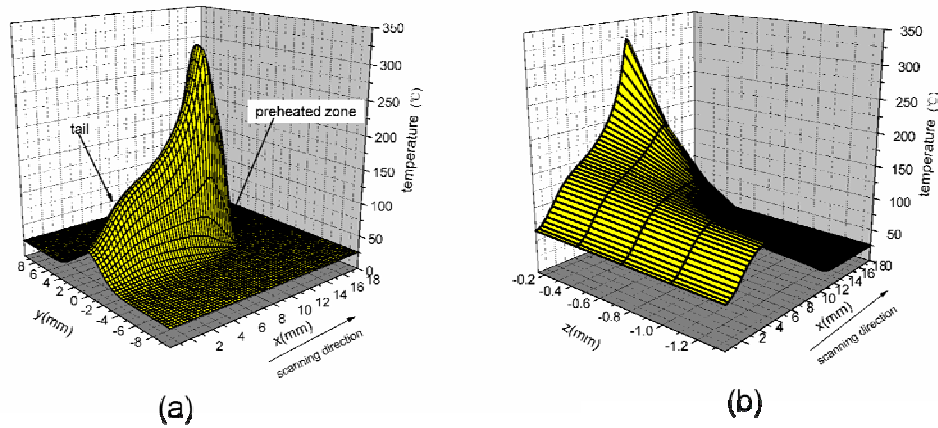

Fig. 3 The temperature distribution in the 304 steel sheet: (a) in xoy plane; (b) in surface yoz plane.

Figure 4 shows the temperature evolution in different depths. It is noticed that the temperature rises rapidly at the metal surface during the laser radiation, while the cooling process is relatively slow due to the thermal conductivity. With the increment of depth, the temperature change rate was decreased.
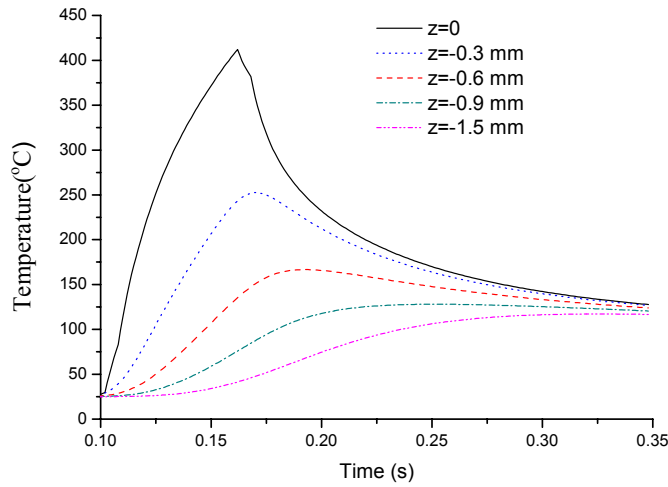

Fig. 4 The temperature evolution as a function of time at different heat penetrating depthes in the 304 steel sheet.

The surface temperature field in x-direction, with and without considering the absorbitivity's temperature dependence, are illustrated in Fig.5. It can be seen that after considering the absorbtivity's temperature dependence, the temperature field changes more obviously and the peak value increase about 6% which is too large to be neglected. The temperature distributions along the z-direction were also calculated and shown in Fig.6. It shows that the temperature change rate could have a maximum variation of about 5 percent if the temperature-dependent absorbance was taken into account. To have a more deep insight into the thermal field changes, the temperature evolutions as a function of time at different depth beneath the
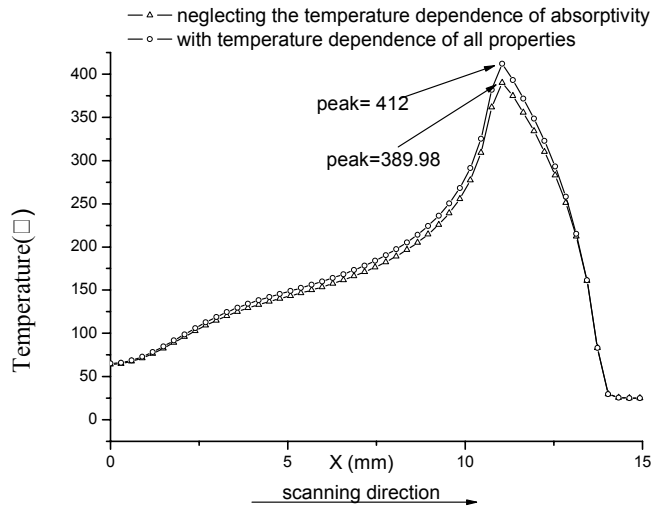
Fig. 5 The temperature distribution along the scanning direction with and without considering the temperature dependence of absorptivity. A large difference of about 6% can be observed.
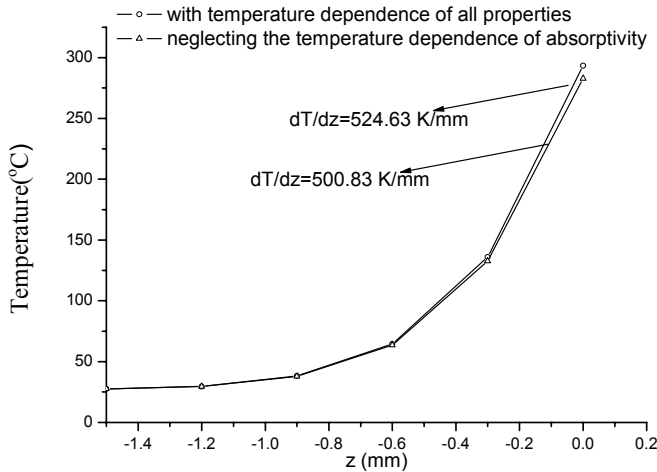

Fig. 6 The temperature distributions along z-direction with and without considering the dependence of absorptivity.

metal surface were depicted in Fig.7. The corresponding temperature evolution curves without considering the absorbitivity's temperature dependence were also illustrated in Fig. 7 for the comparison. we can see not only the noticeable differences between peak temperatures but also the great differences between the temperature change rates. The calculated values for the temperature change rates were listed in Table.2. Therefore, unlike the phase change involved laser-material process for which we can ignore the temperature dependence of the absorbtivity, the temperature dependence of the absorbtivity should be well addressed for the right simulations of thermo-mechanical coupling dominated laser-material processes, such as the laser patterning and laser forming.

Table 2. The temperature change rates calculated with and without considering temperature-dependence of absorptivity

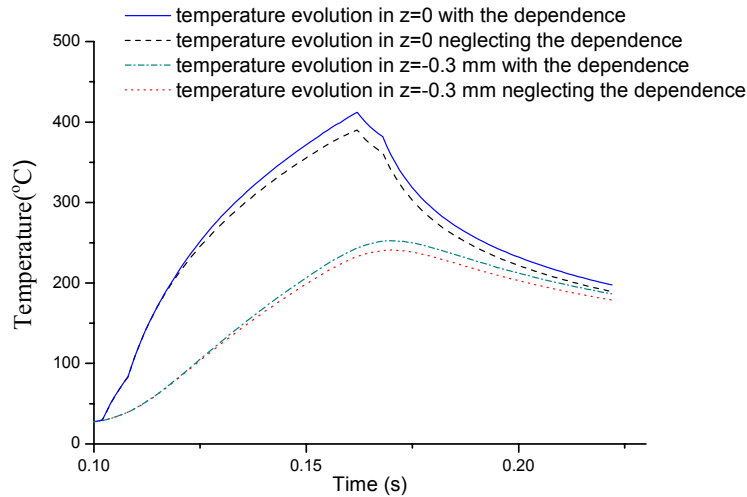| values	Couple of coordinates	Temperature rise velocity (K s^{-1})
Considering the dependence	(0.150, 371.71) (0.155, 389.83)	3624
Neglecting the dependence	(0.150, 355.65) (0.155, 371.95)	3260

Fig. 7 The temperature evolutions in different depths both considering and neglecting the temperature dependence of the abosrbtivity.

CONCLUSIONS

A numerical simulation on the temperature distribution induced by low-energy laser scanning is performed and three-dimensional temperature distribution and temperature evolution as a function of heat penetrating depth in the metal sheet are calculated. It was shown that the temperature dependence of the absorbtivity of the material has great influence on the transient temperature field, the velocity of the temperature rise and the temperature gradient. Therefore, the numerical results indicate that the temperature dependence of laser absorbtivity should be taken into account seriously for tackling the problems on the low-energy laser heating processes, such as the laser forming and laser patterning processes.

REFERENCES

[1] G. F. Chen, X. F. Xu, *Experimental and 3D finite element studies of CW laser forming of thin stainless steel sheets*, J. Manuf. Sci. E-T. Asme., 123, (2001), 66-73.

[2] T. W. Murray, S. Krishnaswamy, *Laser generation of ultrasound in films and coatings,* Appl. Phys. Lett., 74, (1999), 3561-3563.

[3] K. Zhuang, K. Xiao, G. J. Wang, L. Jiang, *Control of thermally induced pattern formation in bilayer metal/polymer films,* Chem. J. Chinese. U., 25, (2004), 157-158.

[4] Z. Ji, S. C. Wu, *FEM simulation of the temperature field during the laser forming of sheet metal*, J. Mater. Process. Tech., 74, (1998), 89-95.

[5] M. Lax, *Temperature rise induced by a laser beam*, J. Appl. Phys., 48, (1977), 3919-3925.

[6] B. J. Bartholomeusz, *Thermal response of a laser-irradiated metal slab*, J. Appl. Phys., 64, (1988), 3815-3819.

[7] P. J. Cheng, S. C. Lin, *Using neural networks to predict bending angle of sheet metal formed by laser*, Int. J. Mach. Tool. Manu., 101, (2000), 260-267.

[8] Y. GF, *Numerical simulation of transient thermal field and residual stress in laser melting process*, Post doctoral thesis, (2002).

[9]   J. C. Conde, F. Lusquinos, P. Gonzalez etc, *Temperature distribution in laser marking,* Vacuum, 64, (2002), 359-366.

[10] M. L. Burgener, R. E. Reedy, Temeprature distributions produced in a two-layer structure by a scanning cw laser or electron beam, J. Appl. Phys., 53, (1982), 4357-4363.

[11] J. P. Hloman, *Heat transfer,* McGraw-Hill, New York (1990).

[12] Y.Ueda, K.Iida, M.saito, A.Okamoto, *Finite element model and residual stress calculation for multi-pass welded joint between a plate and the penetrating pipe*, Modeling of Casting, Welding and Advanced Solidification Processes V, (1991), 219-227.

[13] C. W. Draper, P. Mazzoldi, *Laser surface treatment of metals*, Martinus Nijhoff Publishers, Dordrecht (1986).

[14] W.W. Duley, *Laser processing and analysis of materials,* Plenum Press, New York (1982).